

Effective vector and fermion Higgs portal: A global study

Ankit Beniwal

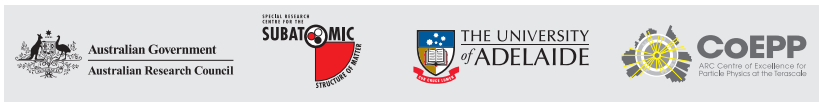
Supervisors: Martin White & Anthony G. Williams

CoEPP and CSSM, Department of Physics,
University of Adelaide, South Australia, Australia

Based on:

- ▶ A. Beniwal, F. Rajec, C. Savage, P. Scott, C. Weniger, M. White and A. G. Williams, PRD, **93**, 115016 (2016), [[arXiv: 1512.06458](#)];
- ▶ Ongoing work with the GAMBIT Collaboration.

CosPA 2016, University of Sydney
November 29, 2016



Outline

1. Dark Matter (DM)
2. Higgs portal
 - ▶ Models
 - ▶ Constraints
 - ▶ Results
3. Global fits
 - ▶ GAMBIT
 - ▶ Bayesian vs Frequentist Inference
 - ▶ Initial scan details
 - ▶ Preliminary results
4. Conclusions

Dark Matter (DM)

- ▶ Accounts for $\sim 27\%$ of the total matter-energy density.¹
- ▶ Has no electromagnetic or strong interactions \implies “dark” and non-luminous.
- ▶ Evidence and properties are inferred from gravitational influences on visible matter, e.g.,
 - ▶ Galactic rotation curves,
 - ▶ Cosmic Microwave Background (CMB),
 - ▶ Gravitational lensing (e.g., Bullet cluster).
- ▶ No viable candidates for DM in the Standard Model (SM) \implies beyond the SM (BSM) candidates.
- ▶ WIMPs are well-motivated DM candidates due to the “WIMP miracle.”

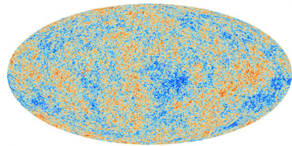


Fig. 1: Cosmic Microwave Background (CMB) as measured by the Planck satellite.



Fig. 2: Distribution of ordinary (red) and dark (blue) matter in the Bullet cluster (1E 0657-56).

¹P. A. R. Ade *et al.*, AAP, 594, A13 (2016), [arXiv: 1502.01589].

Higgs portal

- Models with the following interaction Lagrangian

$$\mathcal{L}_{\text{int}} \supset \frac{1}{\Lambda^n} X^2 \mathbf{H}^\dagger \mathbf{H},$$

where Λ is the EFT cut-off scale, X is the DM field and \mathbf{H} is the SM Higgs doublet.

- X can be a vector (V_μ), Majorana (χ) or Dirac (ψ) fermion. Model Lagrangians are

$$\mathcal{L}_V = \mathcal{L}_{\text{SM}} - \frac{1}{4} W_{\mu\nu} W^{\mu\nu} + \frac{1}{2} \mu_V^2 V_\mu V^\mu - \frac{1}{4!} \lambda_V (V_\mu V^\mu)^2 + \frac{1}{2} \lambda_{hV} V_\mu V^\mu \mathbf{H}^\dagger \mathbf{H},$$

$$\mathcal{L}_\chi = \mathcal{L}_{\text{SM}} + \frac{1}{2} \bar{\chi} (i\cancel{\partial} - \mu_\chi) \chi - \frac{1}{2} \frac{\lambda_{h\chi}}{\Lambda_\chi} \left(\cos \theta \bar{\chi} \chi + \sin \theta \bar{\chi} i \gamma_5 \chi \right) \mathbf{H}^\dagger \mathbf{H},$$

$$\mathcal{L}_\psi = \mathcal{L}_{\text{SM}} + \bar{\psi} (i\cancel{\partial} - \mu_\psi) \psi - \frac{\lambda_{h\psi}}{\Lambda_\psi} \left(\cos \theta \bar{\psi} \psi + \sin \theta \bar{\psi} i \gamma_5 \psi \right) \mathbf{H}^\dagger \mathbf{H}.$$

- In the fermion models, $\cos \theta = 1(0) \implies$ pure scalar (pseudoscalar) and parity conserving (violating) interaction.
- DM is stabilised by imposing an assumed \mathbb{Z}_2 symmetry: $X \rightarrow -X$ for $X \in (V_\mu, \chi, \psi)$.

- ▶ After Electroweak Symmetry Breaking (EWSB),

$$X^2 \mathbf{H}^\dagger \mathbf{H} \rightarrow X^2 \left(\frac{1}{2} v_0^2 + v_0 h + \frac{1}{2} h^2 \right),$$

where $v_0 = 246.22$ GeV is the SM Higgs VEV and h is the physical SM Higgs field.

- ▶ The term $\propto v_0 h X^2$ leads to all the known DM phenomenology.

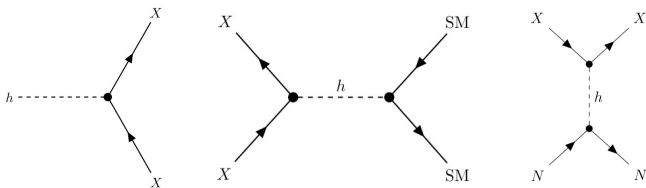


Fig. 3: Methods to look for Higgs portal DM at colliders (left), indirect (center) and direct (right) detection experiments. Here, $N \in (p, n)$ and $SM \in q\bar{q}, l\bar{l}, W^+W^-, ZZ, hh$.

- The physical vector DM mass is

$$m_V = \sqrt{\mu_V^2 + \frac{1}{2} \lambda_{hV} v_0^2}. \quad (1)$$

- If $\sin \theta \neq 0$ in the fermion models \implies non-mass-type contributions. Redefine fields by performing a chiral rotation

$$X \rightarrow \exp(i\gamma_5 \alpha/2)X, \quad \bar{X} \rightarrow \bar{X} \exp(i\gamma_5 \alpha/2),$$

where $X \in (\chi, \psi)$ and α is a constant.

- Require coefficients of $\bar{X}i\gamma_5 X \rightarrow 0$ in the real mass basis, leading to the following post-EWSB Lagrangian

$$\mathcal{L}_X = \mathcal{L}_{\text{SM}} + \kappa \bar{X}(i\not{\partial} - m_X)X - \kappa \frac{\lambda_{hX}}{\Lambda_X} (\cos \xi \bar{X}X + \sin \xi \bar{X}i\gamma_5 X) \left(v_0 h + \frac{1}{2} h^2 \right),$$

where $\xi \equiv \theta + \alpha$ and $\kappa = 1/2$ (1) for the Majorana (Dirac) fermion DM.

- The physical fermion DM mass is

$$m_X = \sqrt{\left(\mu_X + \frac{1}{2} \frac{\lambda_{hX}}{\Lambda_X} v_0^2 \cos \theta \right)^2 + \left(\frac{1}{2} \frac{\lambda_{hX}}{\Lambda_X} v_0^2 \sin \theta \right)^2}. \quad (2)$$

Constraints

1. **Relic density:** model's relic density ($\Omega_X h^2$) must match with the Planck (2013) measured value²

$$\Omega_{\text{DM}} h^2 = 0.1199.$$

2. **Higgs invisible width:** require the Higgs invisible branching ratio³

$$\mathcal{BR}(h \rightarrow \bar{X}X) \leq 0.19 \quad (2\sigma \text{ C.L.})$$

3. **Indirect detection (ID):** satisfy constraints from⁴

- ▶ cosmic microwave background (CMB) radiation,
- ▶ combined analysis of 15 dwarf galaxies by Fermi-LAT,
- ▶ projected limits from the Cherenkov Telescope Array (CTA).

In the fermion models, $\cos \xi = 1 \implies$ weak indirect search limits (due to a v^2 -suppressed annihilation cross section).

4. **Direct detection (DD):** constraints from the LUX (2013) and projected XENON1T experiments.⁵

In the fermion models, $\cos \xi = 0 \implies$ weak direct search limits (due to a q^2 -suppressed SI cross section).

²P. A. R. Ade *et al.*, AAP, **571**, A16 (2014), [arXiv: 1303.5076].

³G. Belanger *et al.*, PRD, **88**, 075008 (2013), [arXiv: 1306.2941].

⁴J. M. Cline and P. Scott, JCAP, 03 (2013) 044, [arXiv: 1301.5908]; M. Ackermann *et al.*, PRD, **88**, 082002 (2013), [arXiv: 1503.02641]; H. Silverwood *et al.*, JCAP, 03 (2015) 055, [arXiv: 1408.4131].

⁵D. Akerib *et al.*, PRL, **112**, 091303 (2014), [arXiv: 1310.8214]; E. Aprile *et al.*, JCAP, 04 (2016) 027, [arXiv: 1512.07501].

Results

Vector DM: Low mass range

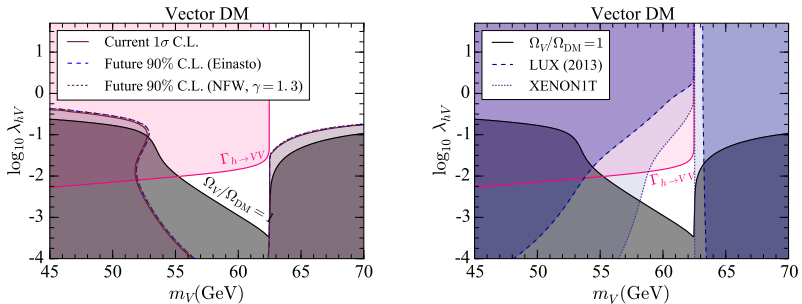


Fig. 4: Indirect (left) and direct (right) search limits in the low mass range.

- ▶ Grey (pink) region: excluded by relic density (Higgs invisible width) constraint.
- ▶ Current ID limits: CMB (WMAP7) + Fermi-LAT (15 dSphs, 6 years);
- ▶ Future ID limits: CMB (Planck) + proj. Fermi-LAT + proj. CTA.

Results

Dirac fermion DM: Low mass range

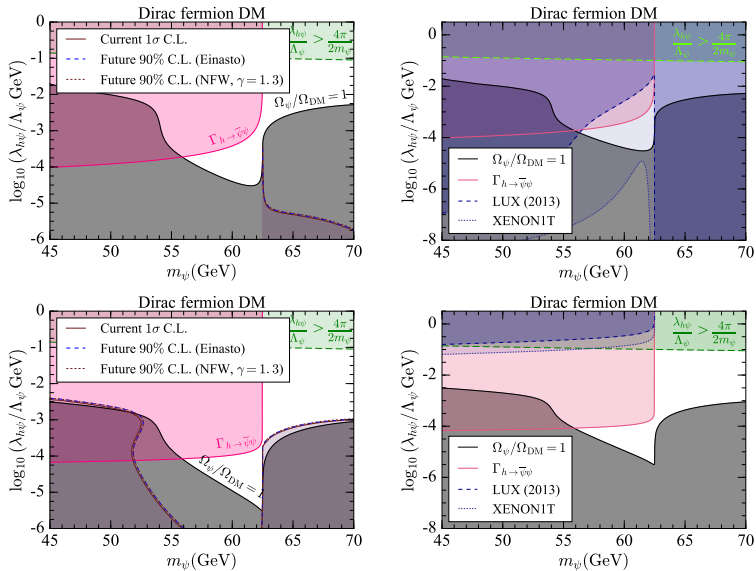


Fig. 5: Indirect (left) and direct (right) search limits in the low mass range when $\cos \xi = 1$ (top) and 0 (bottom).

Global fits

For these simple portal models, we have

- ▶ Combined limits from various DM searches;
- ▶ Overlayed the exclusion limits on top of each other;
- ▶ Showed the allowed and/or excluded regions of the model parameter space.

What if we instead want to

- ▶ Combine *all* constraints consistently (e.g., using a composite likelihood function)?
- ▶ Vary SM, nuclear and astrophysical parameters (i.e., “nuisance parameters”) within their allowed ranges?

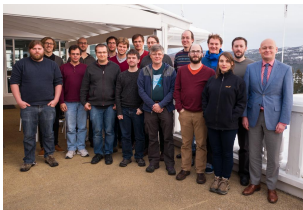
Such questions are addressed by **global studies/fits**.

GAMBIT: The Global And Modular BSM Inference Tool

gambit.hepforge.org

- Fast definition of new datasets and theoretical models
- Plug and play scanning, physics and likelihood packages
- Extensive model database – not just SUSY
- Extensive observable/data libraries
- Many statistical and scanning options (Bayesian & frequentist)
- *Fast* LHC likelihood calculator
- Massively parallel
- Fully open-source

ATLAS	A. Buckley, P. Jackson, C. Rogan, M. White,
LHCb	M. Chrząszcz, N. Serra
Belle-II	F. Bernlochner, P. Jackson
Fermi-LAT	J. Conrad, J. Edsjö, G. Martinez, P. Scott
CTA	C. Balázs, T. Bringmann, J. Conrad, M. White
HESS	J. Conrad
IceCube	J. Edsjö, P. Scott
XENON/DARWIN	J. Conrad, R. Trotta
Theory	P. Athron, C. Balázs, T. Bringmann, J. Cornell, J. Edsjö, B. Farmer, T. Gonzalo, A. Fowlie, J. Harz, S. Hoof, F. Kahlhoefer, A. Krislock, A. Kvællestad, M. Pato, F.N. Mahmoudi, J. McKay, A. Raklev, R. Ruiz, P. Scott, R. Trotta, C. Weniger, M. White, S. Wild



31 Members, 9 Experiments, 4 major theory codes, 11 countries

⁶Slide taken from P. Scott's talk at IDM, Sheffield, July 2016.

Bayesian vs Frequentist Inference

Bayesian inference

- Based on Bayes' theorem

$$p(\boldsymbol{\theta}|\mathcal{D}) = \frac{p(\mathcal{D}|\boldsymbol{\theta})p(\boldsymbol{\theta})}{\int p(\mathcal{D}|\boldsymbol{\theta}')p(\boldsymbol{\theta}') d\boldsymbol{\theta}'},$$

where \mathcal{D} is the data, $\boldsymbol{\theta}$ are the model parameters, $p(\boldsymbol{\theta}|\mathcal{D})$ = posterior PDF, $p(\mathcal{D}|\boldsymbol{\theta}) \equiv \mathcal{L}(\boldsymbol{\theta})$ = likelihood function and $p(\boldsymbol{\theta})$ = prior PDF.

- Marginalised posterior for θ_i is

$$p_m(\theta_i|\mathcal{D}) = \int p(\boldsymbol{\theta}|\mathcal{D}) d\theta_1 \dots d\theta_{i-1} d\theta_{i+1} \dots d\theta_n.$$

- $p_m(\theta_i|\mathcal{D})$ peaks at the region of *highest posterior mass*.

Frequentist inference

- Use a likelihood function $\mathcal{L}(\boldsymbol{\theta})$.
- Profile likelihood for θ_i is

$$\mathcal{L}_p(\theta_i) = \max_{\{\theta_1, \dots, \theta_{i-1}, \theta_{i+1}, \dots, \theta_n\}} \mathcal{L}(\boldsymbol{\theta}).$$

- $\mathcal{L}_p(\theta_i)$ peaks at the region of *highest likelihood*.

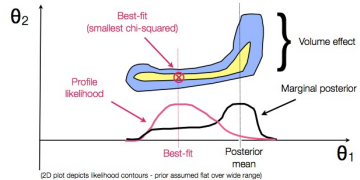


Fig. 6: 1D profile likelihood and marginalised posterior distributions. Figure made by Roberto Trotta.

Initial scan details

Parameter	Range	Prior
m_V (GeV)	[45, 70]	flat
λ_{hV}	$[1.0 \times 10^{-4}, 10]$	log

Table 1: Vector DM model parameters and their ranges.

Parameter	Range	Prior
$m_{\chi, \psi}$ (GeV)	[45, 70]	flat
$\lambda_{h\chi, h\psi} / \Lambda_{\chi, \psi}$ GeV	$[1.0 \times 10^{-6}, 1]$	log
$\cos \xi$	[0, 1]	flat

Table 2: Fermion DM model parameters and their ranges.

Parameter	Central value	Uncertainty	Range	Prior
G_F (GeV $^{-2}$)	1.1663787×10^{-5}	6.0×10^{-12}	$[1.1663769 - 1.1663805] \times 10^{-5}$	flat
α^{-1}	127.940	0.014	[127.898, 127.982]	flat
m_d (GeV) (@ 2 GeV in $\overline{\text{MS}}$)	-	-	$[3.84 - 5.76] \times 10^{-3}$	flat
m_u (GeV) (@ 2 GeV in $\overline{\text{MS}}$)	-	-	$[1.84 - 2.76] \times 10^{-3}$	flat
m_s (GeV) (@ 2 GeV in $\overline{\text{MS}}$)	95×10^{-3}	5.0×10^{-3}	$(80 - 110) \times 10^{-3}$	flat
m_b (GeV) (@ m_b in $\overline{\text{MS}}$)	4.18	0.03	[4.09, 4.27]	flat
m_c (GeV) (@ m_c in $\overline{\text{MS}}$)	1.275	0.025	[1.2, 1.35]	flat
m_t (GeV)	173.34	0.76	[171.06, 175.62]	flat
m_h (GeV)	125.09	0.24	[124.1, 127.3]	flat
σ_s (MeV)	43	8	[19, 67]	flat
σ_l (MeV)	58	9	[31, 85]	flat
ρ_0 (GeV/cm 3)	0.4	0.15	[0.2, 0.8]	flat

Table 3: A list of SM, nuclear and astrophysical parameters included in the initial scan. Except for the ρ_0 likelihood (log-normally distributed), likelihoods for all other parameters were chosen to be *Gaussian*. For the u and d quarks, a Gaussian likelihood was constructed instead from the mass ratios: m_u/m_d and $2m_s/(m_u + m_d)$. The parameters $\sigma_s \equiv m_s \langle N|\bar{s}s|N \rangle$ and $\sigma_l \equiv m_l \langle N|\bar{u}u + \bar{d}d|N \rangle$ where $m_l \equiv (1/2)(m_u + m_d)$ and $N \in (p, n)$ are the strangeness and light quark matrix elements respectively.

Preliminary results: Vector DM

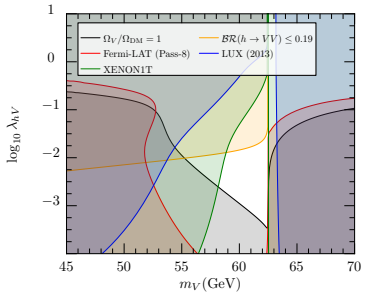


Fig. 7: Results from arXiv: 1512.06458.

Current constraints include:

- ▶ Planck (2015) measured DM relic density;
- ▶ Higgs invisible width (i.e., $BR(h \rightarrow \bar{X}X) \leq 0.19$ @ 2σ C.L.);
- ▶ Fermi-LAT combined analysis of 15 dSphs;
- ▶ XENON100 (2012), SuperCDMS (2014), LUX (2015, 2016) and PandaX (2016).

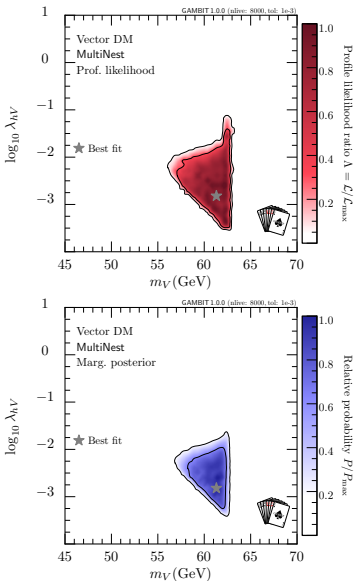


Fig. 8: Preliminary results from GAMBIT.

Preliminary results: Dirac fermion DM

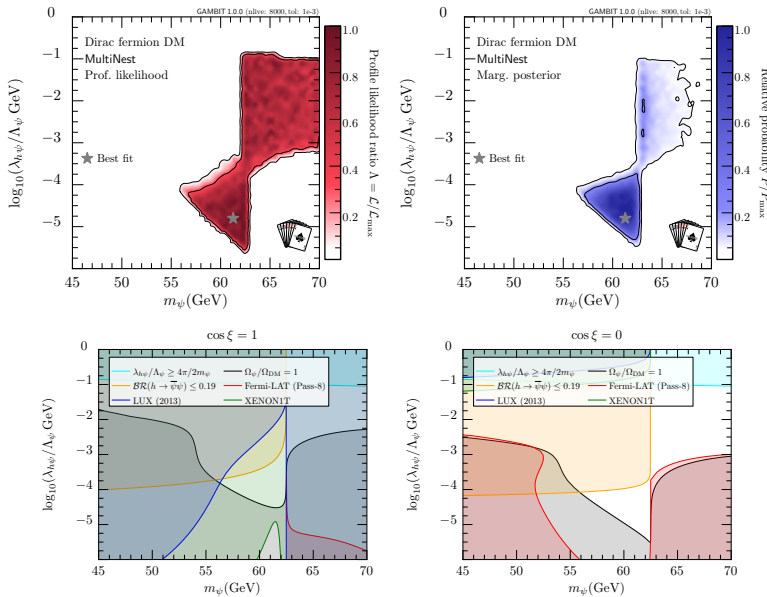


Fig. 9: Comparison of results between GAMBIT (top) for $\cos \xi \in [0, 1]$ and arXiv: 1512.06458 (bottom).

Conclusions

- ▶ Higgs portal models provide rich DM phenomenologies.
- ▶ The combined DM relic density, Higgs invisible width and direct search limits exclude most of the low mass region (except for $m_X \sim m_h/2$).
- ▶ Direct searches are playing, and will continue to play a crucial role in excluding parts of the model parameter space.
- ▶ Indirect searches, although weaker, are also important (particular when the DM-Higgs boson interaction is pure pseudoscalar, i.e., $\cos \xi = 0$).

Coming up:

- ▶ First proper global study of the nonscalar portal models.
-

Backup slides

Results

Scalar DM

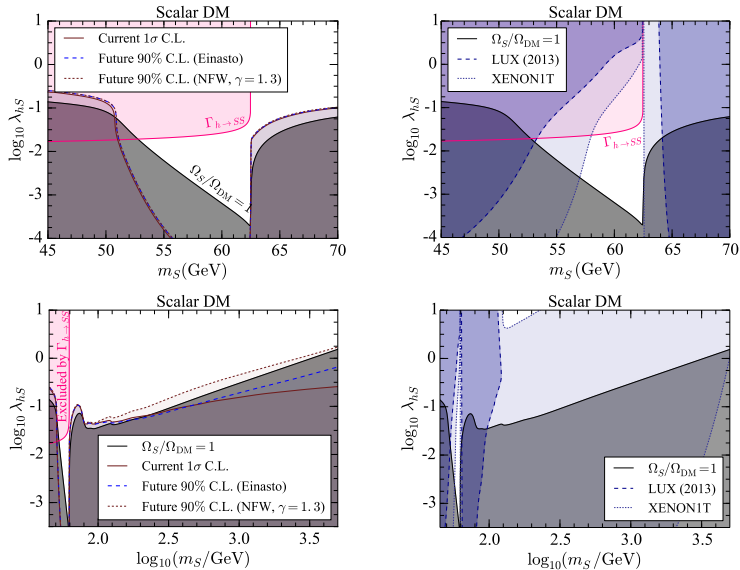


Fig. 10: Indirect (left) and direct (right) search limits in the low (top) and high (bottom) mass range.

Results

Vector DM: High mass range

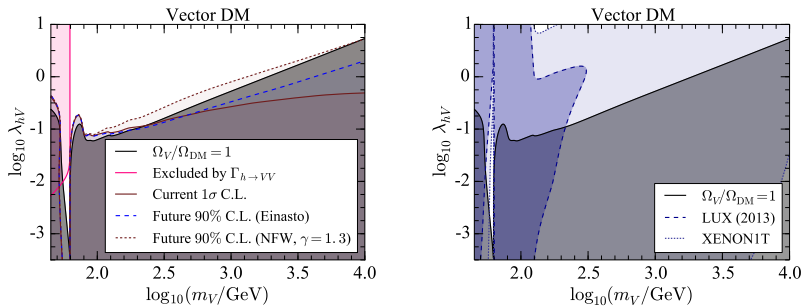


Fig. 11: Indirect (left) and direct (right) search limits in the high mass range.

Results

Dirac fermion DM: High mass range

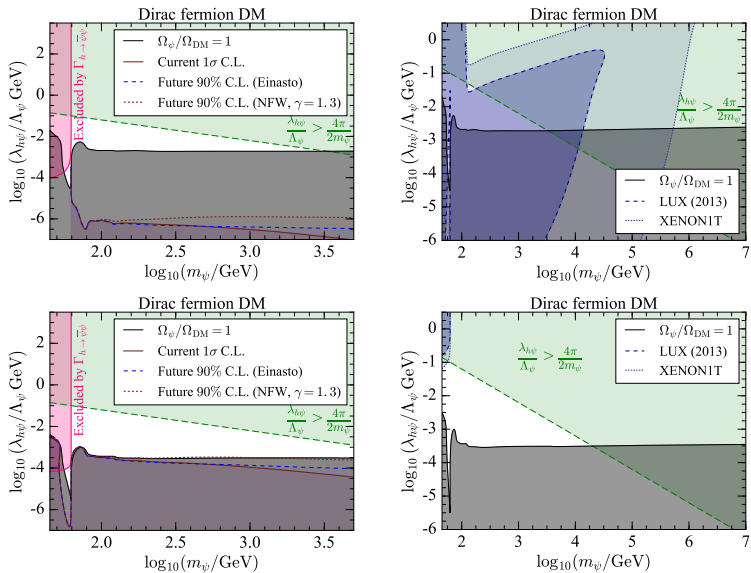


Fig. 12: Indirect (left) and direct (right) search limits in the high mass range when $\cos \xi = 1$ (top) and 0 (bottom).

Results

Majorana fermion DM: Low mass range

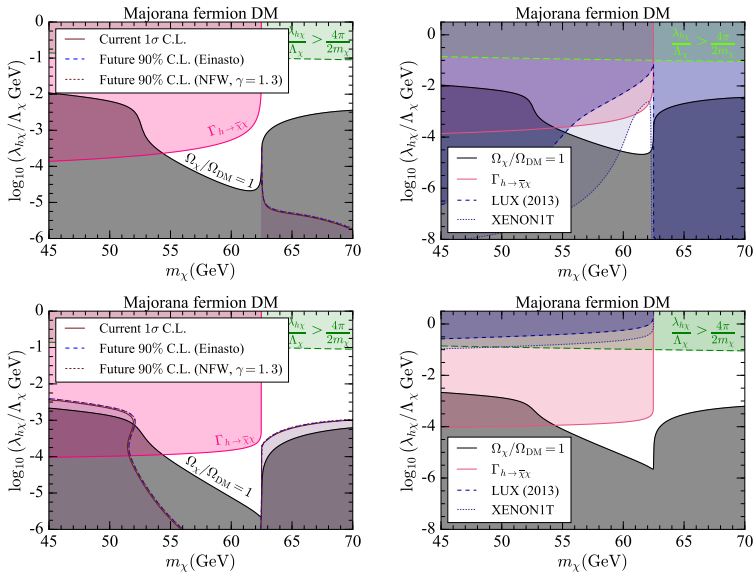


Fig. 13: Indirect (left) and direct (right) search limits in the low mass range when $\cos \xi = 1$ (top) and 0 (bottom).

Results

Majorana fermion DM: High mass range

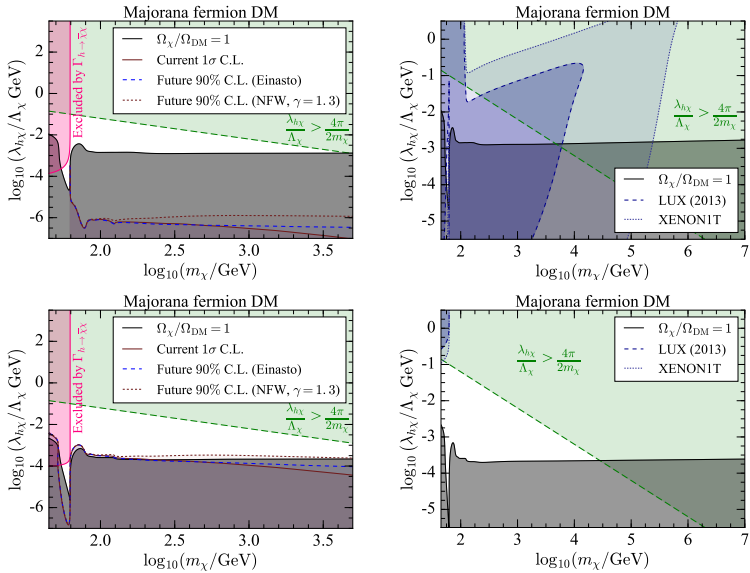


Fig. 14: Indirect (left) and direct (right) search limits in the high mass range when $\cos \xi = 1$ (top) and 0 (bottom).

Preliminary results: Majorana fermion DM

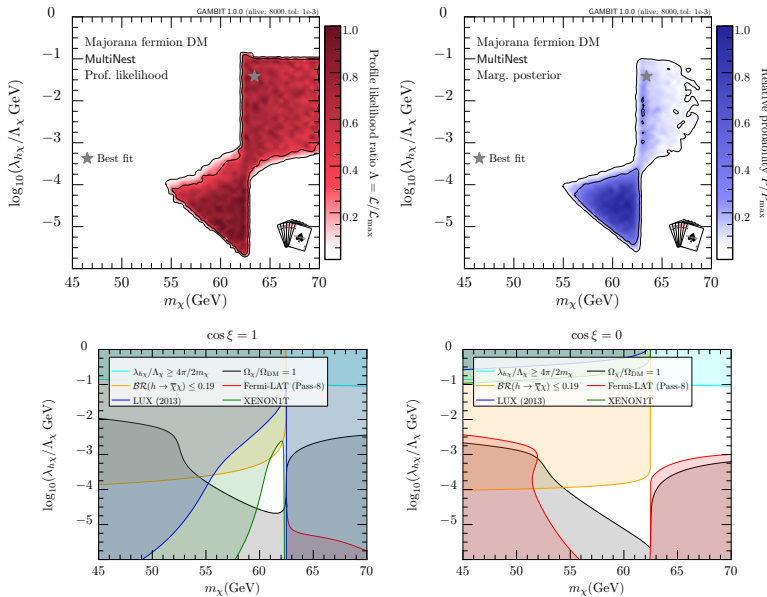


Fig. 15: Comparison of results between GAMBIT (top) for $\cos\xi \in [0, 1]$ and arXiv: 1512.06458 (bottom).